

Valorization of a Levulinic Acid Platform through Electrospinning of Polyhydroxyalkanoate-Based Fibrous Membranes for In Vitro Modeling of Biological Barriers

Anna Lapomarda, Micaela Degli Esposti, Simone Micalizzi, Paola Fabbri, Anna Maria Raspolli Galletti, Davide Morselli,* and Carmelo De Maria*



Cite This: *ACS Appl. Polym. Mater.* 2022, 4, 5872–5881



Read Online

ACCESS |



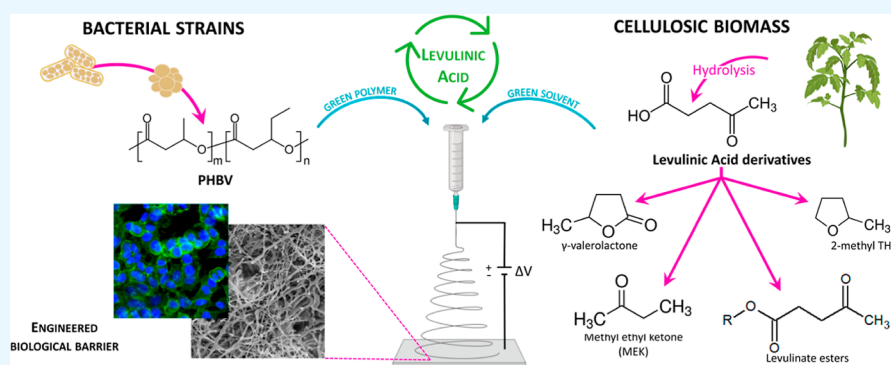
Metrics & More



Article Recommendations



Supporting Information



ABSTRACT: In vitro models of biological barriers provide a reliable tool for investigating the physiopathological processes involved in the development of numerous diseases. Producing sustainable in vitro models obtained from solvents and biopolymers derived from industrial by-products add an important value to this underestimated source of valuable (bio)materials. This work aims at demonstrating the suitability of processing together solvents derived from levulinic acid (LA) (extracted from biomasses) and poly(3-hydroxybutyrate-co-3-hydroxyvalerate) (PHBV) (whose production is facilitated by LA) to produce electrospun membranes as proof-of-concept of a sustainable, engineered biological barrier fully derived from LA as the starting feedstock. The electrospinning process is initially optimized by identifying the most suitable conditions for obtaining self-supporting microporous membranes. In particular, LA-derived solvents (γ -valerolactone, 2-methyltetrahydrofuran, methyl ethyl ketone, and methyl and ethyl levulinate), PHBV concentration, and electrospinning process parameters were investigated. Self-standing and hydrophobic PHBV mats with a micropore size in the range of 1–7 μm and an average elastic modulus of 75 MPa are successfully obtained by using methyl ethyl ketone/formic acid as solvent. Preliminary cell experiments demonstrate that the developed fibrous PHBV mats promote the formation of a confluent monolayer of epithelial cells after 48 h and therefore they can potentially be used to mimic biological epithelial barriers.

KEYWORDS: levulinic acid, PHBV, valorization, electrospinning, biological barrier, green solvents, fibrous membranes

1. INTRODUCTION

The valorization of industrial by-products to produce polymers or additives^{1,2} and green solvents^{3,4} extracted from biomasses can potentially reduce the dependency from non-renewable resources. The identification of fabrication technologies able to process together these biopolymers and green solvents into added-value products offers a valuable approach to further boost their large-scale production and therefore their cost-effective introduction in everyday life.^{5–9}

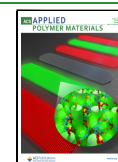
Electrospinning is a versatile and scalable fabrication technology to produce mats of unwoven and randomly oriented fibers. The size of these fibers can range from several nanometers to micrometers.¹⁰ The morphology and the size of the electrospun fibers depend on several parameters including

solution properties (e.g., solvent volatility, polymer concentration, polymer molecular mass, viscosity of the solution), process parameters (e.g., applied voltage, spinneret-collector distance, flow rate), and environmental conditions (e.g., temperature and humidity).^{10,11} Previous studies have shown

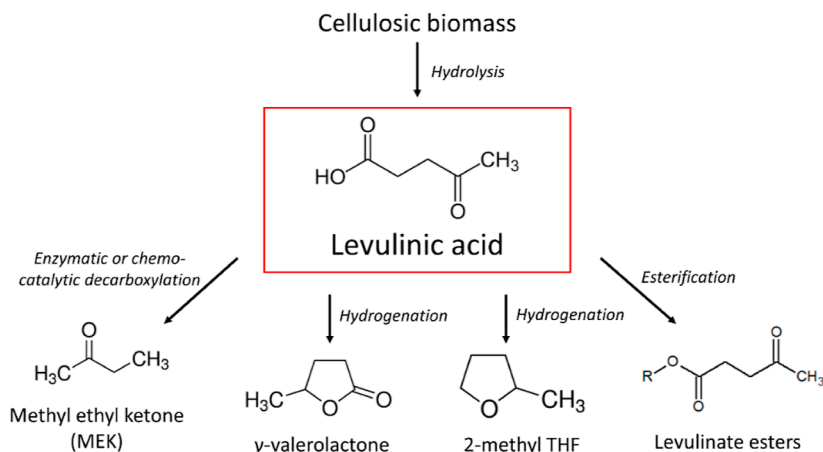
Received: May 4, 2022

Accepted: July 13, 2022

Published: July 25, 2022



Scheme 1. LA-Derived Solvents



that the polymer and the solvent(s) are the most important parameters to control.^{12,13}

The unique capability of producing highly porous mats, with high surface-to-volume ratio, makes electrospinning a suitable method for fabricating scaffolds for a large number of applications in the field of tissue engineering.^{14,15} The stochastic organization of the nanometric electrospun fibers allows, in fact, to mimic the natural arrangement of the structural proteins (e.g., collagen, elastin) of biological extracellular matrix on nano- and microscale.¹⁶ Notably, the presence of an interconnected network of micro-/nanopores makes these electrospun structures valid candidates to reproduce the features of native epithelial barriers (e.g., lung barrier,¹⁷ intestinal barrier¹⁸). Similar to the biological epithelial barrier, in fact, the porous electrospun structures support the exchange of nutrients and the transport of metabolites between two interfaces¹⁹ (such as air–tissue interface, liquid–tissue interface, or liquid–liquid interface).

The composition of the electrospun structures plays a key role on the regulation of the activities of cells that constitute the epithelial barriers. Therefore, the selection of the proper biomaterial is pivotal in this field. Among bio-derived polymers, poly(hydroxyalkanoate)s (PHAs) are a very promising class of fully bio-based thermoplastic polyesters, which are produced by various bacterial strains as intracellular energy storage.²⁰ PHAs are well-known for their high biodegradability in both composting site and open environment without producing any toxic products.^{21,22} These biopolyesters are also known as suitable materials for biomedical applications due to their excellent biocompatibility and bioresorbability.^{23,24} Thanks to these properties, PHAs have recently found applications in other technological fields such as substrates for green electronics and sensors.^{9,24} Among PHAs, poly(3-hydroxybutyrate-co-3-hydroxyvalerate) (PHBV) is one of the most known, thanks to its much higher processability with respect to homopolymer poly(3-hydroxybutyrate)). The valerate block significantly decreases the typical high crystallinity degree of poly(3-hydroxybutyrate) (up to 80%), altering its isotactic stereoregular structure²⁵ and thus making PHBV less stiff and brittle.

The poor solubility of PHAs in organic solvents forces to use halogenated solvents for their solvent-mediated processing as in the case of solvent-casting, spin-coating, and also electrospinning.^{26–29} The use of such toxic solvent for the PHA processing is in contrast with the excellent biodegradability and

biocompatibility that make PHAs one of the most sustainable polymeric materials. Until now, only a few examples of benign solvents have been reported. Most of them are based on weak carboxylic acids as acetic or formic acid (FA)²⁴ that can not only solubilize PHAs but also hydrolyze the ester bond when the solution is stored for several days. Furthermore, these organic acids have a slow evaporation rate, due to the presence of hydrogen bonds, which makes the electrospinnability of the polymeric solution difficult. In order to prevent these drawbacks, these organic acids can be diluted with green organic solvents with higher volatility, hence taking advantage of the properties of both solvents.

In this context, a strategic role is played by solvents derived from levulinic acid (LA, 4-oxopentanoic acid). LA is a bifunctional acid containing both ketonic and carboxylic acid moieties, which can be obtained from both hemicellulosic and cellulosic fractions of biomass. LA can be formed from hemicellulose (mainly xylan) via a three-step process where it is first depolymerized/dehydrated to furfural by an acid catalyst, then furfural is converted to furfuryl alcohol by catalytic hydrogenation, and finally LA is formed from furfuryl alcohol by acid hydrolysis.³⁰ LA can be obtained in a simpler single-step process through the acid-catalyzed hydrothermal conversion of neat C6 sugars or of cellulose and, above all, in waste biomasses.³¹ This hydrothermal conversion involves an initial depolymerization of cellulose into glucose and its subsequent conversion into FA and LA in equimolar amount. Notably, FA and LA belong to the same bio-based production chain, and FA is a valuable co-product of LA industrial synthesis. For this reason, FA has been also recently proposed as benign solvent for electrospinning of PHA-based materials representing a valuable alternative to chlorinated solvents.

LA has been identified by the US Department of Energy as one of the top 12 bio-based building blocks due to its unique chemical versatility which makes it a precursor of many other chemicals with wide market applications.³² Among these, γ -valerolactone (GVL), 2-methyltetrahydrofuran (2MeTHF), methyl ethyl ketone (2-butanone, also known as MEK), methyl levulinate, and ethyl levulinate may show promising properties as co-solvents for electrospinning PHAs (Scheme 1).

GVL is a C5 cyclic ester, and it can be obtained through a catalytic hydrogenation in green medium (e.g., water) of LA. GVL is a green solvent that has shown promising properties as

Table 1. Results of the Electrospinnability Evaluation of PHBV-Based Solutions in Different Solvent Ratios of LA Derivative/FA (GVL/FA, 2MeTHF/FA, MEK/FA, Methyl Levulinate/FA)

| solvent composition | | PHBV concentration (mg mL ⁻¹) | PHBV solubility | electrospinnability | Comments |
|-----------------------------|-------|---|-----------------|---------------------|---|
| solvents | ratio | | | | |
| GVL/FA methyl levulinate/FA | 80:20 | 50 | yes | no | formation of drops rather than fibers |
| | 50:50 | 100 | yes | yes | formation of fibers at the spinneret; however, these coalesce on the collector due to the low volatility of GVL and methyl levulinate |
| 2MeTHF/FA MEK/FA | 50:50 | 50 | yes | no | no fiber formation due to the low concentrated solution |
| | | 100 | yes | no | no fiber formation due to the low concentrated solution |
| | | 200 | yes | yes | formation of short fibers and drops at room temperature due to the gel-like nature. Formation of fibers when electrospun at 60 °C |
| | 40:60 | 200 | yes | yes | formation of fibers at the spinneret; however, these coalesce on the collector due to the low volatility of FA |

bio-fuel, and versatile intermediate for the synthesis of polymeric materials and fine chemicals. The hydrogenation of LA into GVL via heterogeneous catalysis has been deeply investigated and ruthenium-based catalysts show the highest efficiency for this process.³³

By properly tuning the reaction conditions, the hydrogenation of LA or of GVL itself selectively affords the non-polar derivative 2MeTHF. This solvent is a very interesting biomass-derived molecule with a broad range of applications, ranging from bio-fuel to non-ozone-depleting green solvent.³⁴

Another strategic class of LA derivatives is represented by its alkyl esters, which can be obtained by esterification of neat LA or by direct one-pot acid-catalyzed alcoholysis of lignocellulosic biomass.³⁵ The characteristics of alkyl levulinates are influenced by the nature of the adopted alcohol. In particular, they are valuable intermediates for the synthesis of plasticizers, coatings, pharmaceuticals, and bio-surfactants.³⁵ Short chain methyl and ethyl levulinates are promising bio-based additives for gasoline and diesel fuel, respectively.³⁶

MEK, is another valuable LA derivative characterized by an excellent low boiling point. MEK can be obtained through an enzymatic³⁷ or chemo-catalytic decarboxylation³⁸ of LA, both green approaches which represent a sustainable alternative to its synthesis from fossil-based resources.

The adoption of FA in combination with the above reported LA-derived solvents for PHA solubilization represents an innovative and complete valorization of LA production chain, which opens the way to a fully bio-based fabrication process.

Since the last two decades, LA has been also proposed as organic acid co-substrate of glucose-like carbon sources for the production of PHAs.³⁹ The replacement of primary carbon sources and organic acid co-substrates, which can be derived from renewable forestry resources, is one of the strategies proposed for significant reduction of PHA copolymer production costs.⁴⁰ Recently, LA has been also proposed as valuable and cost-effective feeding, which can be used in conjunction with other low-cost co-substrates improving the convenience of PHA production, and can positively affect cell growth and the properties of the obtained PHAs.^{40–42} In particular, it was observed that the content of 3-hydroxyvalerate (3HV) block in PHBV can be controlled by the initial concentration of LA in the fermentation media.⁴²

This work aims at showing the high versatility of LA as a bio-based platform by screening the electrospinnability of PHBV in green solvents for obtaining added-value fibrous products fully derived from LA as the starting feedstock. In

particular, a potential application of the developed porous structures as epithelial barrier for tissue engineering is investigated. Short-term cell experiments using A549 adenocarcinomic human alveolar basal epithelial cells have been performed to assess the suitability of PHBV electrospun structures for developing an in vitro model of lung epithelium.

2. MATERIALS AND METHODS

2.1. Purification and Characterization of PHBV. Custom grade PHBV (Merck, Italy) was used after an accurate purification process to remove very low molecular mass fractions, fermentation residues, and/or possible additives that can alter the results. In particular, as received the PHBV was solubilized in CHCl₃ at 60 °C, filtered through Celite, and precipitated in a large excess of refrigerated methanol, as described elsewhere.⁴³

The purified PHBV was characterized by proton nuclear magnetic resonance (¹H NMR) in order to confirm the absence of any possible synthesis impurities and to determine the molar content of 3HV units. The spectrum of purified PHBV was recorded using a Bruker FT-NMR AVANCE III HD 600 MHz spectrometer and the molar content of 3HV units was determined by integral ratio between 3-hydroxybutyric (3HB) units and 3HV units. The spectrum was recorded at room temperature using approximately 10 mg of purified polymer dissolved in 0.85 mL of deuterated chloroform (99.8 at. % D, 0.03% v/v of TMS, Merck, Italy). Data were processed with Bruker TopSpin software, version 4.0.7. From the recorded ¹H NMR spectrum (Figure S1A, Supporting Information) the molar content of 3HV unit is of approx. 22%.

Molecular mass as peak molecular weight (M_p) of 252,700 g mol⁻¹, number average molecular weight (M_n) of 109,200 g mol⁻¹, weight average molecular weight (M_w) of 319,800 g mol⁻¹, and dispersity index (DI) of electrospun PHBV were determined after the purification procedure by size exclusion chromatography (SEC) (chromatograms in Figure S1B, Supporting Information). An Agilent 1260 Infinity instrument (G1322A 1260 Degasser, G1310B 1260 Isocratic Pump, G1316A 1260 TCC Thermostatted Column Compartment, G1362A 1260 RID Reflective Index Detector, G1328C 126 Manual Injector) was used for the chromatographic analysis. RID and column compartment were thermostatically controlled at 35 °C. The instrument was equipped with a PLgel MiniMIX-A column (20 μm particle size, 4.6 mm × 250 mm) coupled with a Tosoh TSKgel SuperMultipore HZ-M column (4 μm particle size, 4.6 mm × 150 mm). Columns were preceded by a low dispersion in-line filter (frit porosity 0.2 μm). CHCl₃ (HPLC grade, Merck, Italy) was used as the mobile phase at a flow rate of 0.2 mL min⁻¹ and toluene (HPLC grade, Merck, Italy) was used as the flow marker (0.2 μL mL⁻¹) with a run time of 37 min. Results were processed with Agilent GPC/SEC software, version A.02.01 using a calibration curve obtained with monodispersed polystyrene (PS) standards (EasiCal PS-1 Agilent kit: 6,570,000; 2,403,000; 602,000; 276,600; 117,700; 67,600; 27,060; 9820; 2790; and 580 g mol⁻¹).

2.2. Preparation of Electrospinnable PHBV Solutions and Optimization of the Electrospinning Process.

Purified PHBV was dissolved in GVL (Merck, $T_b = 205\text{ }^\circ\text{C}$), 2MeTHF (Carlo Erba, $T_b = 80.2\text{ }^\circ\text{C}$), MEK (Merck, $T_b = 79.7\text{ }^\circ\text{C}$), ethyl levulinate (Merck, $T_b = 200\text{ }^\circ\text{C}$), and methyl levulinate (Merck, $T_b = 190\text{ }^\circ\text{C}$) and stirred for 12 h at $60\text{ }^\circ\text{C}$ at a concentration of 90 mg mL^{-1} . The effect of the polymer solubility in the solvents was initially investigated through a qualitative visual inspection. When aggregates of PHBV were visible in the medium after stirring, PHBV concentration and/or the solvent were not considered adequate for solubilizing PHBV. Therefore, the concentration of PHBV was initially lowered by a stepwise dilution to 50 and to 20 mg mL^{-1} (Table S1, Supporting Information). If PHBV flakes were still visible after the dilutions, different volumes of FA (Sigma-Aldrich, $T_b = 100.8\text{ }^\circ\text{C}$) were added to the solutions/mixtures due to its capability of dissolving PHBV²⁴ (Table 1). Notably, the concentration of PHBV was further tuned in order to obtain suitable solutions for electrospinning (Table 1). The solutions were therefore stirred at $60\text{ }^\circ\text{C}$ for 12 h when PHBV was completely dissolved and used for electrospinning.

The warm solutions were subsequently loaded into a 10 mL glass syringe equipped with a metallic needle, and electrospun using a Linari electrospinning apparatus. To prevent the sol-to-gel transition of the PHBV solutions at room temperature, the syringe was inserted into a digitally controlled heating system to maintain the temperature of PHBV solutions at $60\text{ }^\circ\text{C}$ during the electrospinning process (Figure S2, Supporting Information). This allowed keeping the solutions in a liquid state, avoiding the clogging of the spinneret, and the consequent failure of the electrospinning process. A non-sticky aluminum foil (Reynolds Wrap, USA) was used as the collector. The electrospinning process was optimized by identifying the most suitable needle size (ranging from 21 to 23 G), voltage (ranging from 20 to 50 kV), the feeding rate (ranging from 0.6 to 2 mL h^{-1}), and spinneret-to-collector distance (ranging from 10 to 20 cm) that allowed the fiber formation.

2.3. Physicochemical Characterization of the PHBV Electrospun Structures. Peak molecular weight (M_p), number average molecular weight (M_n), weight average molecular weight (M_w), and DI of electrospun PHBV were determined by SEC before and after polymeric solution preparation and electrospinning, using the same experimental procedure previously described.

The architecture of the PHBV mats was investigated by field emission scanning electron microscopy (FE-SEM) using a Mira3 electron microscope (Tescan), applying an accelerating voltage of 5 kV. The samples were coated with graphite (approx. 10 nm) by the electrodeposition method (using a Quorum Q150R ES) to impart electrical conduction before the analysis. The pore size was determined by ImageJ using FE-SEM images of the electrospun structures.

Contact angle of the electrospun structures was measured at room temperature with the sessile drop method using a tensiometer (Biolin Scientific) and a computer-based processing system. Ultrapure water was used in the experiment. Contact angle was obtained by averaging the results of nine droplets placed at different locations of the surface of the electrospun structure.

The mechanical properties of the electrospun structures were determined by a uniaxial tensile test using a Z005 Zwick–Roell tester machine equipped with a 100 N load cell. Rectangular-shaped samples ($n = 5$) measuring $5\text{ mm} \times 40\text{ mm}$ and with a thickness of $50\text{ }\mu\text{m}$ were die-cut from the electrospun structures and tested at a strain rate of $10\%\text{ min}^{-1}$, with a grip-to-grip separation of 20 mm. The elastic modulus, yield strength, yield strain, ultimate strength, and ultimate strain and toughness were derived from the engineering stress–strain curves. In particular, the elastic modulus and toughness were calculated as the slope of the linear region at strain values of 0.1–0.4%, and as the area under the stress–strain curve, respectively. Additionally, the hysteresis of the electrospun structures ($n = 5$) was investigated through a uniaxial cyclic tensile test (three cycles) using the same parameters as described above. In this case, the samples were stretched up to 1% strain.

2.4. Cytocompatibility Assay. A549 adenocarcinomic human alveolar basal epithelial cells [Interlab Cell Line Collection (ICLC) IRCCS San Martino Policlinico Hospital, Italy] were grown in a 75 cm^2 cell culture flask using Dulbecco's modified Eagle's medium high glucose (Merck, Italy), supplemented with 1% penicillin/streptomycin (Merck, Italy), 1% non-essential amino acids (Merck, Italy), 4 mM L-glutamine (Merck, Italy), and 10% fetal bovine serum (FBS, Merck, Italy). The cells were incubated under standard culture conditions at $37\text{ }^\circ\text{C}$ in a 95% humidified air containing 5% CO_2 atmosphere. Cell culture medium was changed every 2–3 days and were passaged at >80% confluence.

Disk-shaped samples (10 mm diameter, $50\text{ }\mu\text{m}$ thickness) were die-cut from the electrospun structure and used for in vitro assay. The samples were initially sterilized in ethanol 70% (Sigma-Aldrich) for 20 min and subsequently exposed to UV light for 40 min (20 min each side). Afterward, the samples were washed in phosphate-buffered saline (PBS, Lonza). Prior to cell seeding, the samples were placed into a 48-well plate and coated with a sterile solution of gelatin 1% w/v (type A, from porcine skin, Sigma-Aldrich) for 30 min in a humidified incubator with 5% CO_2 . Afterward, the gelatin solution was aspirated and the samples were preconditioned in the cell culture medium overnight. A549 cells were subsequently seeded on top of the samples (15×10^4 cells per sample) and incubated at $37\text{ }^\circ\text{C}$ in a humidified incubator with 5% CO_2 . Additionally, A549 cells were seeded onto tissue culture plate ($n = 2$) as control.

Cell viability of A549 cells seeded onto the electrospun structures ($n = 3$) at 48 h and was assessed by an Alamar Blue cell viability assay (Sigma-Aldrich, Italy) according to the manufacturer's instructions. At the predefined timepoints, the 10% Alamar Blue was added to the cell culture medium and the samples were incubated at $37\text{ }^\circ\text{C}$ in the dark for 2.5 h. Subsequently, the fluorescence of cell medium was measured spectrophotometrically (Synergy H1, microplate reader, BioTek) at an excitation wavelength of 560 nm and an emission wavelength of 590 nm.

Cell morphology of A549 cells at 48 h was investigated by 4',6-diamidino-2-phenylindole (DAPI)/phalloidin staining. At 48 h, the seeded electrospun samples ($n = 2$) were fixed in 4% paraformaldehyde (Sigma-Aldrich) for 30 min at room temperature and subsequently washed two times with PBS (Lonza). Before staining, samples were permeabilized with 0.01% Triton X-100 (Merck, Italy) in PBS for 5 min, washed two times with PBS, and blocked with 5% FBS in PBS for 30 min at room temperature. Then, the samples were first incubated in Alexa Fluor 488 phalloidin (Thermo Fisher, Italy) diluted 1:400 in 1% bovine serum albumin at room temperature for 45 min. After washing twice with PBS, a DAPI solution (Molecular Probes) ($1\text{ }\mu\text{g mL}^{-1}$ in PBS) was added to the samples and incubated for 10 min at room temperature. After three washes with PBS, the samples were observed using a Nikon A1 confocal fluorescence microscope.

2.5. Statistical Analysis. Unless stated otherwise, data are expressed as mean \pm standard deviation. Statistically significant differences among samples were determined by the Student *t* test. Statistical significance was accepted at $p < 0.05$, which is indicated in the figures with the symbol (*).

3. RESULTS AND DISCUSSION

The first step to achieve the formation of a homogeneous fibrous mat is to find a suitable solvent, or a solvent mixture, capable of dissolving the selected polymer. Concurrently, the solvent(s) should be highly volatile to promote the fibers to dry during the fling-time from the spinneret to the collector. Thus, the solubility of PHBV was initially tested in several solvents derived from LA (GVL, 2MeTHF, MEK, ethyl levulinate, and methyl levulinate) in order to obtain PHBV solutions suitable to produce self-standing electrospun mats.

An initial visual screening was performed to identify the most suitable PHBV concentration and type of solvent for electrospinning. When a partial polymer dissolution was

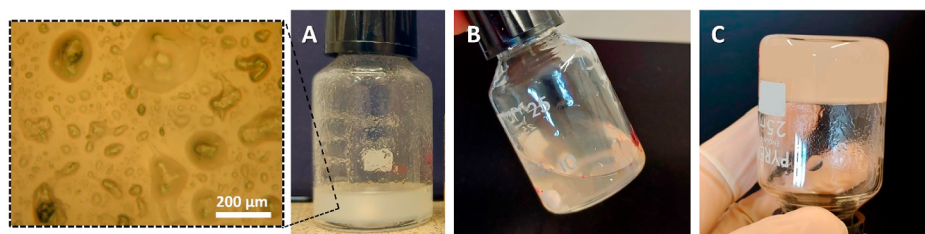


Figure 1. (A) Representative pictures of PHBV dissolved in 2MeTHF at 60 °C (inset: image acquired with an optical microscope). (B) PHBV dissolved in 2MeTHF/FA mixture at 60 °C. (C) PHBV dissolved in 2MeTHF/FA mixture at room temperature.

Table 2. Process Parameters Used to Electrospin PHBV in 2MeTHF/FA and MEK/FA

| solvent composition | | PHBV concentration (mg mL ⁻¹) | DC voltage (kV) | spinneret-to-collector distance (cm) | flow rate (mL h ⁻¹) | spinneret size (μm) | syringe temperature (°C) | duration (h) |
|---------------------|-------|---|-----------------|--------------------------------------|---------------------------------|---------------------|--------------------------|--------------|
| solvents | ratio | | | | | | | |
| 2MeTHF/FA | 50:50 | 200 | 20 | 15 | 1 | 400 | 60 | 3 |
| MEK/FA | 50:50 | | | | | | | |

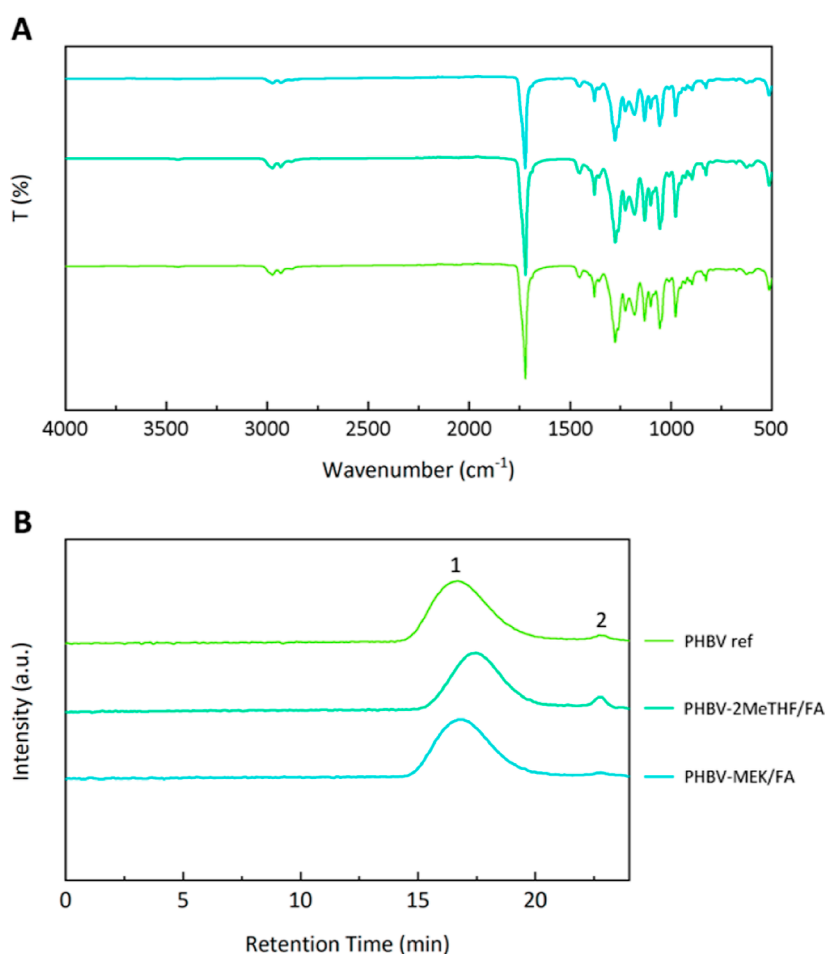


Figure 2. (A) FT-IR spectra and (B) SEC chromatograms of the as-recovered PHBV after the purification process and fibers obtained by electrospinning using 2MeTHF/FA and MEK/FA as solvent mixtures. In the chromatograms, the main fraction of the polymeric chains is indicated as peak 1 and the secondary fraction as peak 2.

observed after 12 h stirring at 60 °C, the solvent was not considered suitable to dissolve PHBV (tested concentrations: 20, 50, and 90 mg mL⁻¹) (Table S1, Supporting Information). From this initial screening, PHBV resulted to be soluble only in ethyl levulinate. This solution appeared translucent without any residual insolubilized PHBV. However, the high boiling temperature of this solvent ($T_b = 200$ °C) prevented the

formation of fiber on the collector and therefore ethyl levulinate was not used for further characterization. On the other hand, a partial solubility of PHBV was observed in GVL, 2MeTHF, MEK, and methyl levulinate, respectively. In order to improve the PHBV solubility in these solvents, FA was added in different volume ratios as reported in Table 1. As shown in Figure 1, the addition of FA to 2MeTHF successfully

enhanced the solubility of PHBV (Figure 1A,B). The solutions appeared less turbid and no insoluble PHBV residues were visible using an optical microscope after 12 h stirring at 60 °C (Figure 1B).

Despite the addition of FA to the LA-based solvents improves the solubility of PHBV, all the polymeric solutions underwent sol-to-gel transition at room temperature (as shown in Figure 1C). This phenomenon negatively affects the electrospinnability of the solution, and it prevents the formation of the fiber under the effect of the electric field during the electrospinning process due to dominant surface tension forces. Therefore, a custom-made heating system for the syringe (Figure S2, Supporting Information) was developed to maintain the polymeric solutions in a liquid state (at 60 °C) during the electrospinning process. Although the heating system strongly improved the electrospinnability of all the PHBV LA derivative/FA solutions, only the 2MeTHF/FA and MEK/FA media allowed suitable performance in terms of electrospinnability of PHBV. When solutions of PHBV in methyl levulinate and GVL/FA were electrospun, the fibers tended to coalesce upon the collector due to the low volatility of the solvents. We hypothesize that this might be due to the high boiling point of methyl levulinate ($T_b = 190$ °C) and GVL ($T_b = 205$ °C) that makes these solutions less volatile than 2MeTHF/FA and MEK/FA.

Considering all these aspects, the most suitable formulations optimized for electrospinning are indicated in Table 2 together with the setting parameters used to electrospin them. Notably, in order to compare the results in terms of mat architecture, the same process parameters were used to electrospin PHBV-based solutions in 2MeTHF/FA and MEK/FA.

The obtained electrospun fibers have been analyzed by FT-IR and SEC in order to identify any possible degradation of the polymeric chains that might take place during the electrospinning process due to the interaction with the used solvents under high voltage. FT-IR spectra of the as-obtained PHBV from the purification process and the PHBV after electrospinning with different solvents do not show any significant difference (Figure 2A). The typical FT-IR signals (assignments in the Supporting Information) of the molecular structure of PHBV do not change, indicating that the primary structure of the polymer is not chemically modified.

SEC chromatograms (Figure 2B) clearly show that after the electrospinning process the molecular mass of the polymer processed by 2MeTHF/FA is decreased probably due to the hydrolysis of a small portion of the ester bonds, which can be catalyzed by FA when the temperature is increased up to 60 °C for a long time and/or under high voltage. On the other hand, when MEK/FA is used as solvent a negligible variation of molecular mass is observed.

Specifically, the values of M_p , M_n , M_w , and DI of PHBV calculated from peak 1 (in Figure 2B) are summarized in Table 3. Considering M_n , which is the parameter more affected by low molecular mass fractions, a small reduction of approx. 3% is observed. This variation in PHA-based materials may be due to the non-synthetic origin of these polymers as observed on similar systems and for this reason commonly accepted.⁴³ On the other hand, a significant variation is observed when 2MeTHF/FA is used as solvent. As expected, the overall reduction of the molecular mass leads to an increase of the intensity of peak 2 (secondary fraction) in accordance to Figure 2B.

Table 3. Peak Molecular Weight (M_p), Number Average Molecular Weight (M_n), Weight Average Molecular Weight (M_w), and DI (Calculated as M_w/M_n) as Determined by Gel Permeation Chromatography

| sample | M_p (g mol ⁻¹) | M_n (g mol ⁻¹) | M_w (g mol ⁻¹) | DI |
|-----------|------------------------------|------------------------------|------------------------------|------|
| PHBV_ref | 252,700 | 109,200 | 319,800 | 2.93 |
| 2MeTHF/FA | 127,500 | 69,800 | 163,400 | 2.34 |
| MEK/FA | 226,800 | 105,700 | 282,300 | 2.67 |

The architecture of electrospun PHBV mats produced with 2MeTHF/FA and MEK/FA have been investigated with FE-SEM (Figure 3A1,A2,B1,B2). Under the same operative conditions, different PHBV mats were produced. An irregular and porous structure was observed in the PHBV mats using 2MeTHF/FA as solvent (Figure 3A1,A2), whereas a random orientation of flat ribbon-like fibers with undulated edges was obtained using MEK/FA as solvent (Figure 3B1,B2). In this case, PHBV fibers are less merged than the fibers obtained in 2MeTHF/FA, showing an interconnected network of micropores. The complete or partial fusion of PHBV fibers might be a consequence of not complete evaporation of the solvent mixture from the ejected charged jet. This phenomenon is more noticeable when 2MeTHF/FA is used as solvent, where we contextually have the reduction of PHBV molecular mass combined to its partial hydrolysis in FA at 60 °C. This can additionally explain the impossibility of detaching the PHBV mats from the non-sticky aluminum collector when 2MeTHF/FA is used as solvent. Moreover, the brittleness of the obtained non-freestanding mats by 2MeTHF/FA makes this material unsuitable for the goal of this work and thus it was not further characterized.

On the other hand, homogeneous, microporous, and freestanding PHBV mats with remarkably large dimensions (20 cm diameter) were successfully electrospun using MEK/FA as solvent (Figure 3C). The distribution of the measured pore size of the micropores is reported in Figure 3D. In particular, these mats show micropores whose size predominantly ranges from 1 to 7 μm and an average distribution mainly centered at approx. 2 μm .

The water contact angle was measured to investigate the wettability of the electrospun PHBV mats. As expected, microporous PHBV mats exhibited a contact angle of $114.3 \pm 6.2^\circ$ in good agreement with the known hydrophobic nature of PHBV.⁴⁴

The mechanical properties of PHBV electrospun mats in MEK/FA were assessed by uniaxial tensile tests. A representative stress–strain curve for PHBV fibrous mat (Figure 4A) exhibits a two-slope shape, with an initial steep linear region followed by a marked plastic deformation. The mean values of the mechanical properties calculated from the curves are summarized in Figure 4B. These results are in line with other previous studies based on electrospun PHBV membranes, which have been used also for supporting the growth of functional esophageal epithelial cells.^{44–47} In vitro models of alveolar epithelial barriers usually are based on soft substrates (hundreds of kPa), also more rigid materials have been successfully tested (up to tens of MPa).^{48,49} The mechanical behavior of PHBV electrospun mats in MEK/FA on loading and unloading cycles was also investigated (Figure 4C). The hysteresis in each loading–unloading cycle was calculated as the area of each cycle and represents the energy lost per cycle. The hysteresis decreases in the initial cycle (p -

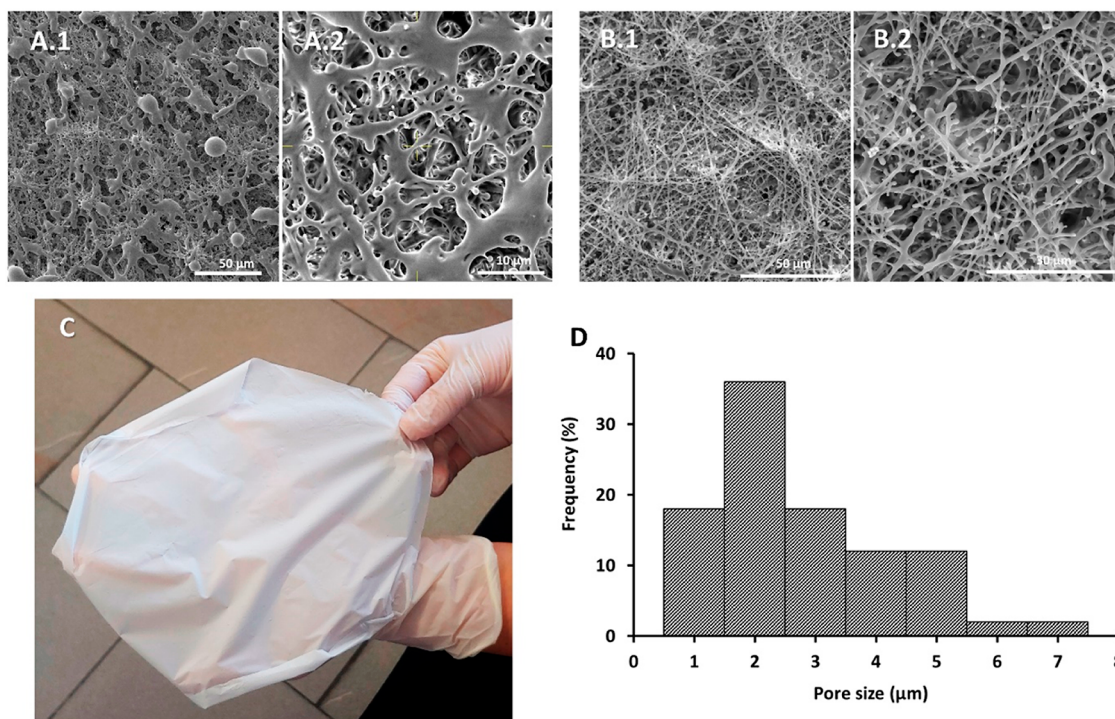


Figure 3. FE-SEM images of PHBV electrospun fibers using (A.1 and A.2) 2MeTHF/FA and (B.1 and B.2) MEK/FA as solvent. (C) Picture of the prepared freestanding electrospun PHBV mat in MEK/FA. (D) Pore size distribution of micropores in the PHBV mats electrospun using MEK/FA as solvent.

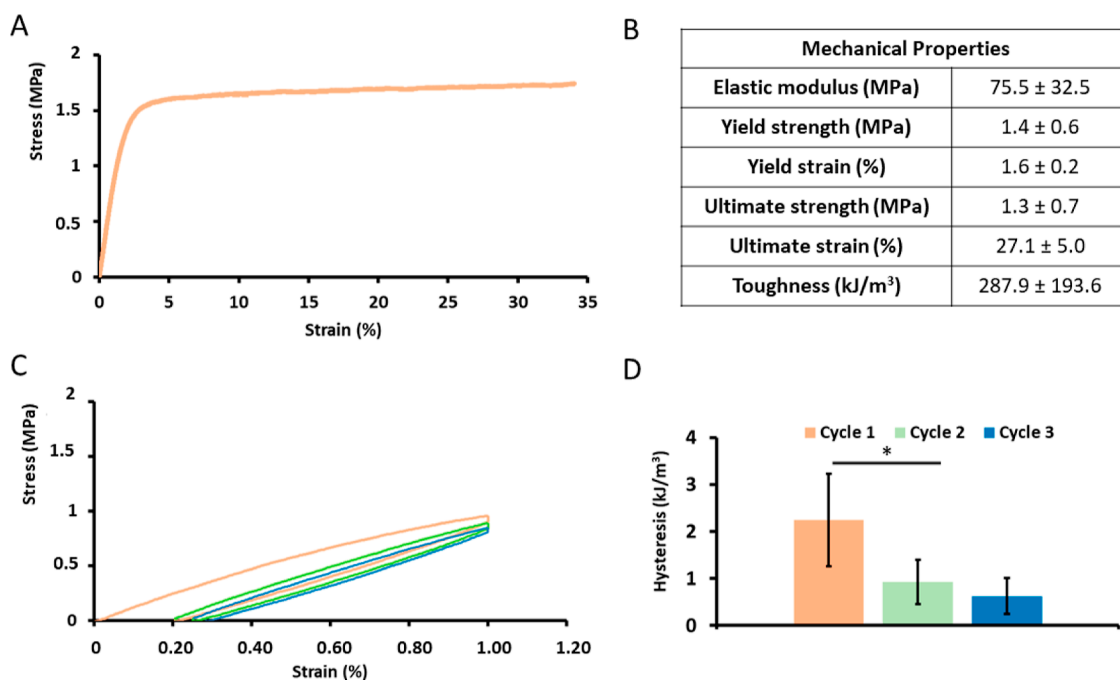


Figure 4. (A) Representative stress–strain curve. (B) Measured mechanical properties of PHBV fibrous mats in MEK/FA. (C) Cyclic strain test (1% × 3 cycles) of PHBV fibrous mats in MEK/FA. (D) Measured hysteresis at each cycle.

value < 0.05) and remains constant for the remaining cycles (Figure 4D).

To investigate the application of the obtained electrospun PHBV mats in MEK/FA as sustainable substrates for in vitro models of biological barriers, a cell viability assay was performed using A549 adenocarcinomic human alveolar basal epithelial cells. This cell line has been extensively used as a

model of the alveolar epithelial barrier.^{49,50} As shown in Figure 5A, no significant difference in the metabolic activity was observed on PHBV mats compared to the control at 48 h. The morphology of A549 cells was investigated by staining cell nuclei with DAPI and actin fibers of the cytoskeleton with phalloidin. As shown in Figure 5B,C, at 48 h the characteristic rounded shape specific of confluent A549 cells is observed.⁴⁸

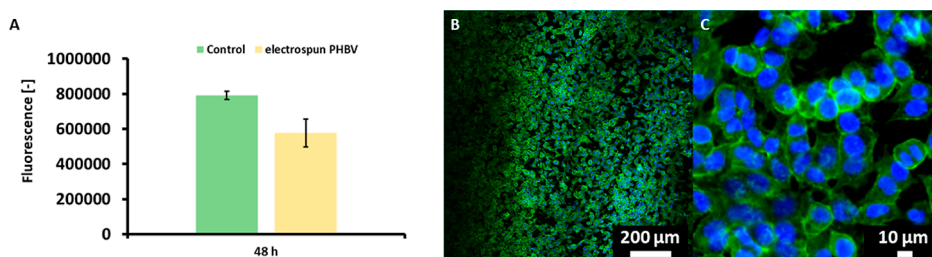


Figure 5. (A) Viability assay of A549 cells on PHBV mats in MEK/FA at 48 h. (B,C) Confocal images of A549 cells cultured for 48 h and stained with DAPI (blue, nuclear stain) and phalloidin (green, actin fibers).

At this timepoint, cells adhere and proliferate, forming a confluent monolayer of epithelial cells on the surface of the PHBV mat. Together these assays demonstrate that the developed PHBV mats in MEK/FA do not negatively affect the viability of A549 cells, and they promote cell adhesion and proliferation of epithelial cells.

4. CONCLUSIONS

In vitro models of biological barriers (e.g., lung epithelium, intestinal epithelium) provide an important benchmark for studying the physiopathological processes (e.g., nutrient and metabolite exchange, interactions with external virus or bacteria) involved in the development of several diseases (e.g., respiratory tract infections and carcinomas). These models represent a reliable platform for a more rapid identification of the most customizable pharmaceutical therapies for their treatment.

The valorization of sustainable and renewable biopolymers and solvents derived from industrial by-products into engineered biological barriers provide an important added-value to this class of (bio)materials. This study shows the first attempt to obtain sustainable electrospun membranes with potential application as an engineered biological barrier, which can be derived from LA as the starting feedstock.

Preliminary experiments were performed to identify the most suitable LA-derived solvents (GVL, 2MeTHF, MEK, methyl levulinate, and ethyl levulinate) and PHBV concentration for obtaining homogeneous solutions processable by electrospinning. To enhance the solubility of PHBV in the LA derivative solvents, FA (co-product of LA industrial synthesis) was added at various volume ratios obtaining binary solvents. Among the tested solutions, PHBV (200 mg mL⁻¹) in MEK/FA (volume ratio 50:50) proved to be the most suitable for the goal of this work.

The electrospinning process was further optimized by identifying the optimal process parameters, and a customized heating system to maintain the PHBV solution in MEK/FA in the liquid phase (at 60 °C) was designed and developed on purpose. Large dimension (20 cm diameter) and self-standing mats, with micropore size between 1 and 7 μm, were successfully electrospun. These mats show irregular and flat ribbon-like fibers that are partially merged. Moreover, these mats show an elastic modulus of 75.5 ± 32.5 MPa for this polymer and a hydrophobic contact angle of 114.3 ± 6.2°, which is comparable to other electrospun PHBV mats reported in the literature. Cell experiments demonstrated that the developed fibrous PHBV mats do not negatively alter cell viability of A549 adenocarcinomic human alveolar basal epithelial cells, which adhere and proliferate on the surface

of the PHBV mats forming a confluent monolayer of epithelial cells after 48 h.

Globally, all these results show for the first time the great potential of converting sustainable solvents and biopolymers, both derived from LA as the starting feedstock, into added-value microporous membranes that can potentially be used as sustainable in vitro models of biological barriers. Moreover, the reported findings open a way of processing PHBV by green solvent not only in electrospinning but also for other solvent-mediated processing approaches.

■ ASSOCIATED CONTENT

Supporting Information

The Supporting Information is available free of charge at <https://pubs.acs.org/doi/10.1021/acsapm.2c00721>.

¹H NMR spectrum and related signal assignments, GPC chromatogram of PHBV, summary of the performed electrospinning experiments, picture of the used electrospinning apparatus, and FT-IR assignments (PDF)

■ AUTHOR INFORMATION

Corresponding Authors

Davide Morselli – Department of Civil, Chemical, Environmental, and Materials Engineering (DICAM), Università di Bologna, 40131 Bologna, Italy; National Interuniversity Consortium of Materials Science and Technology (INSTM), 50121 Firenze, Italy; orcid.org/0000-0003-3231-7769; Email: carmelo.demaria@unipi.it

Carmelo De Maria – Department of Information Engineering, University of Pisa, 56122 Pisa, Italy; Research Center 'E. Piaggio', University of Pisa, 56122 Pisa, Italy; orcid.org/0000-0002-1368-3571; Email: davide.morselli6@unibo.it

Authors

Anna Lapomarda – Department of Information Engineering, University of Pisa, 56122 Pisa, Italy; Research Center 'E. Piaggio', University of Pisa, 56122 Pisa, Italy; orcid.org/0000-0002-8041-8970

Micaela Degli Esposti – Department of Civil, Chemical, Environmental, and Materials Engineering (DICAM), Università di Bologna, 40131 Bologna, Italy; National Interuniversity Consortium of Materials Science and Technology (INSTM), 50121 Firenze, Italy; orcid.org/0000-0002-4513-8527

Simone Micalizzi – Department of Information Engineering, University of Pisa, 56122 Pisa, Italy; Research Center 'E. Piaggio', University of Pisa, 56122 Pisa, Italy; orcid.org/0000-0001-7178-0209

Paola Fabbri – Department of Civil, Chemical, Environmental, and Materials Engineering (DICAM), Università di Bologna,

40131 Bologna, Italy; National Interuniversity Consortium of Materials Science and Technology (INSTM), 50121 Firenze, Italy; orcid.org/0000-0002-1903-8290

Anna Maria Raspolli Galletti – Department of Chemistry and Industrial Chemistry, University of Pisa, 56124 Pisa, Italy; orcid.org/0000-0002-0622-844X

Complete contact information is available at:
<https://pubs.acs.org/10.1021/acsapm.2c00721>

Author Contributions

The manuscript was written through contributions of all authors. All authors have given approval to the final version of the manuscript.

Funding

This study was supported by the Italian Ministry of University and Research (MUR) under the PRIN Project “Development and promotion of the levulinic acid and carboxylate platforms by the formulation of novel and advanced PHA-based biomaterials and their exploitation for 3D printed green electronics applications” grant 2017FWC3WC.

Notes

The authors declare no competing financial interest.

ACKNOWLEDGMENTS

A.L., S.M., and C.D.M. also acknowledge the support of Additive Manufacturing CrossLab of the Department of Information Engineering of the University of Pisa.

REFERENCES

- (1) Sinisi, A.; Degli Esposti, M.; Toselli, M.; Morselli, D.; Fabbri, P. Biobased Ketal-Diester Additives Derived from Levulinic Acid: Synthesis and Effect on the Thermal Stability and Thermo-Mechanical Properties of Poly(vinyl chloride). *ACS Sustainable Chem. Eng.* **2019**, *7*, 13920–13931.
- (2) Sinisi, A.; Degli Esposti, M.; Braccini, S.; Chiellini, F.; Guzman-Puyol, S.; Heredia-Guerrero, J. A.; Morselli, P.; Fabbri, P. Levulinic Acid-Based Bioplasticizers: a Facile Approach to Enhance the Thermal and Mechanical Properties of Polyhydroxyalkanoates. *Mater. Adv.* **2021**, *2*, 7869–7880.
- (3) Antonetti, C.; Licursi, D.; Fulignati, S.; Valentini, G.; Raspolli Galletti, A. M. New Frontiers in the Catalytic Synthesis of Levulinic Acid: from Sugars to Raw and Waste Biomass as Starting Feedstock. *Catalysts* **2016**, *6*, 196.
- (4) Antonetti, C.; Licursi, D.; Raspolli Galletti, A. M. New Intensification Strategies for the Direct Conversion of Real Biomass into Platform and Fine Chemicals: What Are the Main Improvable Key Aspects? *Catalysts* **2020**, *10*, 961.
- (5) Lapomarda, A.; De Acutis, A.; Chiesa, I.; Fortunato, G. M.; Montemurro, F.; De Maria, C.; Mattioli Belmonte, G.; Gottardi, R.; Vozzi, G. Pectin-GPTMS-based Biomaterial: Toward a Sustainable Bioprinting of 3D Scaffolds for Tissue Engineering Application. *Biomacromolecules* **2019**, *21*, 319–327.
- (6) Lapomarda, A.; Cerqueni, G.; Geven, M. A.; Chiesa, I.; De Acutis, A.; De Blasi, M.; Montemurro, G.; De Maria, C.; Mattioli-Belmonte, M.; Vozzi, G. Physicochemical Characterization of Pectin-Gelatin Biomaterial Formulations for 3D Bioprinting. *Macromol. Biosci.* **2021**, *21*, 2100168.
- (7) Lapomarda, A.; Pulidori, E.; Cerqueni, G.; Chiesa, I.; De Blasi, M.; Geven, M. A.; Montemurro, C.; Duce, C.; Mattioli-Belmonte, M.; Tiné, M. R.; Vozzi, G.; De Maria, C. Pectin as Rheology Modifier of a Gelatin-Based Biomaterial Ink. *Materials* **2021**, *14*, 3109.
- (8) Fortunato, G. M.; Da Ros, F.; Bisconti, S.; De Acutis, A.; Biagini, F.; Lapomarda, A.; Magliaro, G.; De Maria, C.; Montemurro, F.; Bizzotto, D.; Braghetta, P.; Vozzi, G. Electrospun Structures Made of

a Hydrolyzed Keratin-Based Biomaterial for Development of In Vitro Tissue Models. *Front. Bioeng. Biotechnol.* **2019**, *7*, 174.

(9) Bittolo Bon, S.; Chiesa, I.; Morselli, D.; Degli Esposti, M.; Fabbri, P.; De Maria, C.; Foggi Viligiardi, L.; Morabito, A.; Giorgi, G.; Valentini, L. Printable smart 3D architectures of regenerated silk on poly(3-hydroxybutyrate-co-3-hydroxyvalerate). *Mater. Des.* **2021**, *201*, 109492.

(10) Bhardwaj, N.; Kundu, S. C. Electrospinning: a Fascinating Fiber Fabrication Technique. *Biotechnol. Adv.* **2010**, *28*, 325–347.

(11) Teo, W. E.; Ramakrishna, S. A Review on Electrospinning Design and Nanofibre Assemblies. *Nanotechnology* **2006**, *17*, R89.

(12) Uyar, T.; Besenbacher, F. Electrospinning of Uniform Polystyrene Fibers: The effect of Solvent Conductivity. *Polymer* **2008**, *49*, 5336–5343.

(13) Shenoy, S. L.; Bates, W. D.; Frisch, H. L.; Wnek, G. E. Role of chain entanglements on fiber formation during electrospinning of polymer solutions: good solvent, non-specific polymer-polymer interaction limit. *Polymer* **2005**, *46*, 3372–3384.

(14) Hasan, A.; Memic, A.; Annabi, N.; Hossain, M.; Paul, A.; Dokmeci, M. R.; Dehghani, A.; Khademhosseini, A. Electrospun Scaffolds for Tissue Engineering of Vascular Grafts. *Acta Biomater.* **2014**, *10*, 11–25.

(15) Lim, S. H.; Mao, H. Q. Electrospun Scaffolds for Stem Cell Engineering. *Adv. Drug Delivery Rev.* **2009**, *61*, 1084–1096.

(16) Han, D.; Gouma, P. I. Electrospun Bioscaffolds that Mimic the Topology of Extracellular Matrix. *Nanomed. Nanotechnol. Biol. Med.* **2006**, *2*, 37–41.

(17) Morris, G. E.; Bridge, J. C.; Brace, L. A.; Knox, A. J.; Aylott, J. W.; Brightling, C. E.; Ghaemmaghami, F. R.; Rose, F. R. A. J. A Novel Electrospun Biphasic Scaffold Provides Optimal Three-Dimensional Topography for In Vitro Co-Culture of Airway Epithelial and Fibroblast Cells. *Biofabrication* **2014**, *6*, 035014.

(18) Patient, J. D.; Hajiali, H.; Harris, K.; Abrahamsson, B.; Tannergren, C.; White, L. J.; Ghaemmaghami, F. R.; Williams, P. M.; Roberts, C. J.; Rose, F. R. A. J. Nanofibrous Scaffolds Support a 3D In Vitro Permeability Model of the Human Intestinal Epithelium. *Front. Pharmacol.* **2019**, *10*, 456.

(19) Khorshidi, S.; Solouk, A.; Mirzadeh, H.; Mazinani, S.; Lagaron, J. M.; Sharifi, S.; Ramakrishna, S. A review of key challenges of electrospun scaffolds for tissue-engineering applications. *J. Tissue Eng. Regen. Med.* **2016**, *10*, 715–738.

(20) Li, Z.; Yang, J.; Loh, X. J. Polyhydroxyalkanoates: Opening Doors for a Sustainable Future. *NPG Asia Mater.* **2016**, *8*, No. e265.

(21) Numata, K.; Abe, H.; Iwata, T. Biodegradability of Poly(hydroxyalkanoate) Materials. *Materials* **2009**, *2*, 1104–1126.

(22) Álvarez-Chávez, C. R.; Edwards, S.; Moure-Eraso, R.; Geiser, K. Sustainability of Bio-based Plastics: General Comparative Analysis and Recommendations for Improvement. *J. Clean. Prod.* **2012**, *23*, 47–56.

(23) Bon, S.; Chiesa, I.; Degli Esposti, M.; Morselli, D.; Fabbri, P.; De Maria, C.; Morabito, L.; Coletta, R.; Calamai, M.; Pavone, F. S.; Tonin, R.; Morrone, A.; Giorgi, G.; Valentini, L. Carbon Nanotubes/Regenerated Silk Composite as a Three-Dimensional Printable Bio-Adhesive Ink with Self-Powering Properties. *ACS Appl. Mater. Interfaces* **2021**, *13*, 21007–21017.

(24) Brunetti, L.; Degli Esposti, M.; Morselli, D.; Boccaccini, A. R.; Fabbri, P.; Liverani, L. Poly(hydroxyalkanoate)s meet benign solvents for electrospinning. *Mater. Lett.* **2020**, *278*, 128389.

(25) Hobbs, J. K.; McMaster, T. J.; Miles, M. J.; Barham, P. J. Cracking in spherulites of poly(hydroxybutyrate). *Polymer* **1996**, *37*, 3241–3246.

(26) Yun, S. I.; Gadd, G. E.; Latella, B. A.; Lo, V.; Russell, R. A.; Holden, P. J. Mechanical Properties of Biodegradable Polyhydroxyalkanoates/Single Wall Carbon Nanotube Nanocomposite Films. *Polym. Bull.* **2008**, *61*, 267–275.

(27) Xu, P.; Yang, W.; Niu, D.; Yu, M.; Du, M.; Dong, W.; Chen, P.; Jan Lemstra, P.; Ma, P. Multifunctional and Robust Polyhydroxyalkanoate Nanocomposites with Superior Gas Barrier, Heat Resistant

and Inherent Antibacterial Performances. *Chem. Eng. J.* **2020**, *382*, 122864.

(28) Kaniuk, Ł.; Krysiak, Z. J.; Metwally, S.; Stachewicz, U. Osteoblasts and fibroblasts attachment to poly(3-hydroxybutyric acid-co-3-hydroxyvaleric acid) (PHBV) film and electrospun scaffolds. *Mater. Sci. Eng., C* **2020**, *110*, 110668.

(29) Liu, C.; Noda, I.; Chase, D. B.; Zhang, Y.; Qu, J.; Jia, M.; Ni, J. F.; Rabolt, J. F. Crystallization Retardation of Ultrathin Films of Poly[(R)-3-hydroxybutyrate] and a Random Copolymer Poly[(R)-3-hydroxybutyrate-co-(R)-3-hydroxyhexanoate] on an Aluminum Oxide Surface. *Macromolecules* **2019**, *52*, 7343–7352.

(30) Yan, K.; Wu, G.; Lafleur, T.; Jarvis, C. Production, Properties and Catalytic Hydrogenation of Furfural to Fuel Additives and Value-Added Chemicals. *Renewable Sustainable Energy Rev.* **2014**, *38*, 663–676.

(31) Licursi, D.; Antonetti, C.; Fulignati, S.; Corsini, A.; Boschi, N.; Raspolli Galletti, A. M. Smart Valorization of Waste Biomass: Exhausted Lemon Peels, Coffee Silverskins and Paper Wastes for the Production of Levulinic Acid. *Chem. Eng. Trans.* **2018**, *65*, 637–642.

(32) Bozell, J. J.; Petersen, G. R. Technology development for the production of biobased products from biorefinery carbohydrates—the US Department of Energy's "Top 10" revisited. *Green Chem.* **2010**, *12*, 539–554.

(33) Raspolli Galletti, A. M.; Antonetti, C.; Ribechini, E.; Colombini, M. P.; Nasso, N.; Bonari, E. From Giant Reed to Levulinic Acid and Gamma-Valerolactone: a High Yield Catalytic Route to Valeric Biofuels. *Appl. Energy* **2013**, *102*, 157–162.

(34) Pace, V.; Hoyos, P.; Castoldi, L.; Domínguez de María, P.; Alcántara, A. R. 2-Methyltetrahydrofuran (2-MeTHF): A Biomass-Derived Solvent with Broad Application in Organic Chemistry. *ChemSusChem* **2012**, *5*, 1369–1379.

(35) Raspolli Galletti, A. M.; Antonetti, C.; Fulignati, S.; Licursi, D. Direct Alcoholysis of Carbohydrate Precursors and Real Cellulosic Biomasses to Alkyl Levulinates: a critical review. *Catalysts* **2020**, *10*, 1221.

(36) Joshi, H.; Moser, B. R.; Toler, J.; Smith, W. F.; Walker, T. Ethyl Levulinate: a Potential Bio-Based Diluent for Biodiesel which Improves Cold Flow Properties. *Biomass Bioenergy* **2011**, *35*, 3262–3266.

(37) Mehrer, C. R.; Rand, J. M.; Incha, M. R.; Cook, T. B.; Demir, B.; Motagamwala, A. H.; Kim, B. F.; Dumesic, J. A.; Pfleger, B. F. Growth-Coupled Bioconversion of Levulinic Acid to Butanone. *Metab. Eng.* **2019**, *55*, 92–101.

(38) Gong, Y.; Lin, L.; Zhang, B. Generation of Methyl Vinyl Ketone from Oxidation of Levulinic Acid Oxidized by Cupric Oxide Complex. *Chin. J. Chem.* **2012**, *30*, 327–332.

(39) Keenan, T. M.; Tanenbaum, S. W.; Stipanovic, A. J.; Nakas, J. P. Production and Characterization of Poly- β -hydroxyalkanoate Copolymers from Burkholderia cepacia Utilizing Xylose and Levulinic Acid. *Biotechnol. Prog.* **2004**, *20*, 1697–1704.

(40) Ashby, R. D.; Solaiman, D. K. Y.; Strahan, G. D.; Zhu, C.; Tappel, R. C.; Nomura, C. T. Glycerine and levulinic acid: Renewable co-substrates for the fermentative synthesis of short-chain poly-(hydroxyalkanoate) biopolymers. *Bioresour. Technol.* **2012**, *118*, 272–280.

(41) Ashby, R. D.; Solaiman, D. K. Y. Levulinic Acid: a Valuable Platform Chemical for the Fermentative Synthesis of Poly-(Hydroxyalkanoate) Biopolymers. *ACS Symp. Ser.* **2018**, *1310*, 339–354.

(42) Ashby, R. D.; Solaiman, D. K. Y.; Nuñez, A.; Strahan, G. D.; Johnston, D. B. Burkholderia sacchari DSM 17165: a Source of Compositionally-Tunable Block-Copolymeric Short-Chain Poly-(Hydroxyalkanoates) from Xylose and Levulinic Acid. *Bioresour. Technol.* **2018**, *253*, 333–342.

(43) Degli Esposti, M.; Chiellini, F.; Bondioli, F.; Morselli, D.; Fabbri, P. Highly Porous PHB-Based Bioactive Scaffolds for Bone Tissue Engineering by In Situ Synthesis of Hydroxyapatite. *Mater. Sci. Eng., C* **2019**, *100*, 286–296.

(44) Yoon, Y. I.; Moon, H. S.; Lyoo, W. S.; Lee, T. S.; Park, W. H. Superhydrophobicity of PHBV Fibrous Surface with Bead-on-String Structure. *J. Colloid Interface Sci.* **2008**, *320*, 91–95.

(45) Bianco, A.; Calderone, M.; Cacciotti, I. Electrospun PHBV/PEO Co-Solution Blends: Microstructure, Thermal and Mechanical Properties. *Mater. Sci. Eng., C* **2013**, *33*, 1067–1077.

(46) Kouhi, M.; Prabhakaran, M. P.; Shamanian, M.; Fathi, M.; Morshed, M.; Ramakrishna, S. Electrospun PHBV Nanofibers Containing HA and Bredigite Nanoparticles: Fabrication, Characterization and Evaluation of Mechanical Properties and Bioactivity. *Compos. Sci. Technol.* **2015**, *121*, 115–122.

(47) Kuppan, P.; Sethuraman, S.; Krishnan, U. M. Poly(3-hydroxybutyrate-co-3-hydroxyvalerate)-based nanofibrous scaffolds to support functional esophageal epithelial cells towards engineering the esophagus. *J. Biomater. Sci., Polym. Ed.* **2014**, *25*, 574–593.

(48) Doryab, A.; Tas, S.; Taskin, M. B.; Yang, L.; Hilgendorff, A.; Groll, J.; Wagner, O.; Schmid, O. Evolution of Bioengineered Lung Models: Recent Advances and Challenges in Tissue Mimicry for Studying the Role of Mechanical Forces in Cell Biology. *Adv. Funct. Mater.* **2019**, *29*, 1903114.

(49) Cei, D.; Doryab, A.; Lenz, A. G.; Schröppel, A.; Mayer, P.; Burgstaller, G.; Nossa, O.; Ahluwalia, A.; Schmid, O. Development of a Dynamic In Vitro Stretch Model of the Alveolar Interface with Aerosol Delivery. *Biotechnol. Bioeng.* **2021**, *118*, 690–702.

(50) Lenz, A. G.; Karg, E.; Lentner, B.; Dittrich, V.; Brandenberger, C.; Rothen-Rutishauser, B.; Schulz, O.; Ferron, G. A.; Schmid, O. A Dose-Controlled System for Air-Liquid Interface Cell Exposure and Application to Zinc Oxide Nanoparticles. *Part. Fibre Toxicol.* **2009**, *6*, 32.

Recommended by ACS

Bill Nye the plastic guy and turning egg cartons into planters

Alex Tullo.

JUNE 27, 2022
C&EN GLOBAL ENTERPRISE

READ 

Chemical firms aim for more ambitious climate goals

Craig Bettenhausen.

JANUARY 11, 2021
C&EN GLOBAL ENTERPRISE

READ 

Celanese to buy ExxonMobil's Santoprene business

Alex Tullo.

JULY 12, 2021
C&EN GLOBAL ENTERPRISE

READ 

Polyurethanes Based on Unmodified and Refined Technical Lignins: Correlation between Molecular Structure and Material Properties

Yun-Yan Wang, Arthur J. Ragauskas, et al.

APRIL 26, 2021
BIOMACROMOLECULES

READ 

Get More Suggestions >